THREE-DIMENSIONAL FLOW REVERSAL IN DROPLETS IN HELE-SHAW CELLS

François gallaire[*a)], Sungyon Lee[**] and Charles Baroud[***]
[*]LFMI, IGM, STI, EPFL, Lausanne, Suisse
[**]Dept. of Mathematics and Applied Mathematics Laboratory, University of California, Los Angeles, CA
[***]LadHyX, Ecole polytechnique, Palaiseau, France

Summary When a droplet of large aspect ratio is held stationary against a mean flow inside a Hele-Shaw cell, a three-dimensional recirculation flow on the drop interface is observed. In contrast to the parabolic flow profile pertaining to Hele-Shaw flows, the velocity profile, displays a 3D-recirculation near the interface, instead of decreasing monotonically away from the mid-plane of the drop. This observation is accounted for by a solutal Marangoni effect modeled through a boundary layer expansion close to the drop interface.

INTRODUCTION

When a fluid flows along a drop of another immiscible fluid, a recirculation pattern is observed inside the droplet, as the consequence of the continuity of shear stress and tangential velocity along the drop interface. This has been first understood for spherical droplets by Hadamard [1] and Rybzinsky [2] in the creeping flow limit. In the presence of surfactants, this recirculation flow further induces a solutocapillary retardation mechanism (Levich [3]) due to surfactant material reorganization along the interface. Similar phenomena are observed in the Hele-Shaw geometry, when the droplet is confined between the channel walls and adopts a pancake like shape. Bush [4] observed a recirculating wake outside a pancake bubble rising due to buoyancy, which he attributed to surfactant redistribution along the interface. While the flow reversal observed by Bush predominantly takes place in-plane (parallel to the top and bottom plates), we describe in this paper an out-of-plane flow reversal which is observed on the drop surface despite the mean unidirectional external flow.

EXPERIMENTAL OBSERVATIONS

As sketched in Figure1a, a pancake droplet confined in a Hele-Shaw cell of height h much smaller than the droplet radius R is held stationary against a mean flow U_o. A simple mechanism is used to hold droplets stationary against the mean flow inside the Hele-Shaw cell [5]: by etching a hole into the top surface of the PDMS channel, the droplet partially enters the indentation, thereby, reducing its overall surface energy. This decrease in surface energy allows the drop to remain "anchored" as long as the drag force from the external flow is less than this surface energy gradient to push the drop out of the hole. A fluorinated oil (FC-40 + 1% surfactant, viscosity $\mu_c \approx 4.1$cP) is used as the carrier fluid. The dispersed phase consists of distilled water of $\mu_d \approx 1$cP together with green-fluorescent beads of diameter 1μm (FluoSpheres, 2% solid) at 5 wt $\%$ as flow tracers, from which quantitative flow measurements are made using a commercial PIV software (DaVis, LaVision). This yields a viscosity ratio of $\lambda = \mu_d/\mu_c = 1/4$.

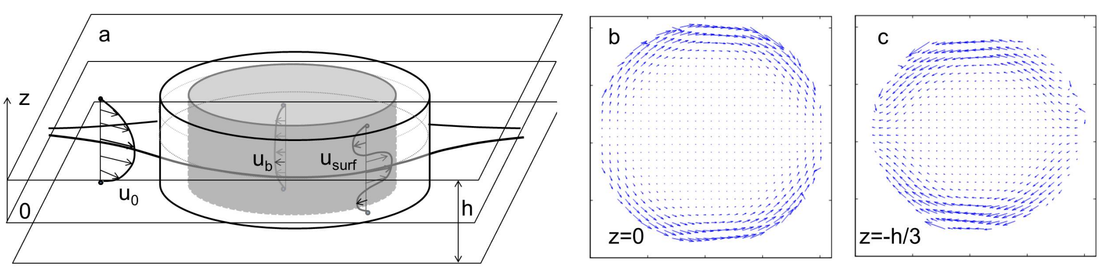

Figure 1. (a) Sketch of the three-dimensional flow reversal (not to scale); (b) velocity field measured at $z = 0$; (c) velocity field measured at $z \approx -h/3$; $h = 50\mu m$, $U_0 = 1mm/s$ and $R = 200\mu m$. Observe the velocity field from left to right in (b) and from right to left in (c).

The PIV visualizations inside the droplet at different different focal planes in Fig. 1b,c show that the center of droplet is nearly immobile in comparison to the fast flow near the boundary of the drop. This fast flow decays over a short length scale that is comparable to the channel height (white region in Fig.1a). Furthermore, the velocity fields at two varying vertical positions $z = 0$ (Fig. 1b) and $z = -15\mu$m (Fig. 1c), respectively, show that the fluid at the drop interface moves in opposite directions depending on z. This signifies that the anchored droplet undergoes a three-dimensional recirculation on the droplet boundary, despite the unidirectional driving flow: the transverse velocity profile $u_{\rm surf}(z)$, instead of decreasing monotonically away from the mid-plane ($z = 0$), switches sign before reaching zero at $z = \pm h/2$.

Figure 2a shows the surface velocity on the drop interface at $x = R, y = \pm R$ for two values of z ($z = 0$ and $z \approx -h/3$) for several values of the channel height h and drop radius R. The surface velocity $u_{\rm surf}(0)$ measured at the mid-plane ($z = 0$) is approximately 32% of U_o, independent of the channel height and drop radius, while the surface velocity $u_{\rm surf}(-h/3)$ measured at

[a)] Corresponding author. E-mail: francois.gallaire@epfl.ch

$z = -10$ and -15 μm for channels of $h = 30$ and 50 μm, respectively, switches sign with a maximum magnitude approximately 13% of the mean external flow. Away from the drop boundary where the fast recirculation flow occurs, the velocity in the center region of the drop is negative and smaller than both u_{surf} and U_{o} in magnitude. The mean velocity that could be measured in the region $r < R/2$ is $0.003U_{\mathrm{o}}$.

MARANGONI MODEL

In order to account for this flow reversal, we model the modification of the interface boundary condition due to the redistribution of surfactant material on the droplet surface. The flow past the droplet causes the surfactants to accumulate on the front of the droplet relative to its rear, creating a surfactant concentration gradient along the droplet interface, which causes in turn a surface tension gradient with a higher surface tension at the rear than at the front [3]. The resultant adverse solutal Marangoni effect pulls along the surface in the opposing direction to the flow. We therefore superimpose to the free-stream carrier flow a prescribed surface tension distribution, ensuring the tail-to-nose surface tension gradient produced by the carrier flow, quantified by a Marangoni number $M = (2\epsilon\Delta\sigma)/(U_{\mathrm{o}}(\mu_c + \mu_d))$, where $\Delta\sigma$ is surface tension variation and $\epsilon = h/R$. In the regime where surface advection dominates over surface diffusion and the adsorption/desorption processes on the interface are not limiting, a natural assumption is to consider a uniform surface tension distribution along z and a linear surfactant concentration gradient in the in-plane direction, as also assumed by Bush [4]. We further simplify the pancake like geometry of the droplet by a flat circular cylinder of radius R and thickness h.

Far from the interface, the separation of scales and low Reynolds number can be exploited to lead to the Hele-Shaw equations, with the classical potential flow solution at leading order in $\epsilon = h/R$. The solution is chosen to match the far-field velocity and to satisfy the impermeability condition on the circular interface. In the process leading to the Hele-Shaw equations, the in-plane diffusion terms are neglected, precluding the imposition of the continuity of tangential velocity and tangential stress. At leading order in ϵ, the flow far from the interface inside the droplet is therefore null. This already implies that the characteristic velocities in the bulk of the droplet are at least ϵ times smaller than U_{o}.

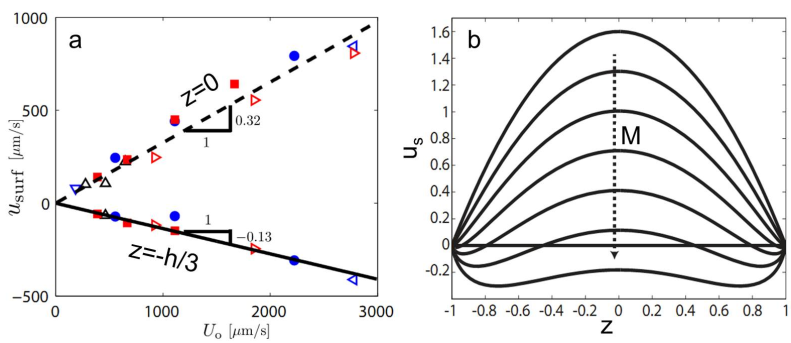

Figure 2. (a) Maximum tangential velocity on the interface u_{surf} on two separate vertical planes versus the mean external flow U_{o} for different values of the channel height and drop radius. (b) Typical velocity profiles $v_s(z)$ obtained from the boundary layer expansion in the vicinity of the droplet surface for an adverse Marangoni effect of non dimensional strength $M = 0, 2, 4, 6, 8, 10, 12$; $\lambda = 1/4$.

In order to fulfill the tangential boundary conditions, a boundary layer expansion (inspired by the boundary layer along a flattened cylinder in a Hele-Shaw cell by Thompson [6]) is introduced close to the boundary where the radial coordinate is rescaled to account for the transverse scale h (white region in Figure 1a). The dominant balance suggests that the tangential velocity component dominates the two other velocity components by at least one order of magnitude. Typical results for a viscosity ratio of $\lambda = 1/4$ are displayed in figure 2b for different values of the retarding soluto-capillary gradient ranging from $M = 0, 2, 4, 6, 8, 10, 12$. In the absence of the Marangoni effect, the maximum surface velocity is computed to be 1.6 in comparison to the value of 2 pertaining to the $\lambda = 0$ case. For moderate Marangoni driving, the flow decelerates until flow reversal appears for $M > 4.23$ near the wall. At $M = 8.7$, a maximum velocity of 0.3 and a minimum of -0.08 compatible with our findings (see Fig. 1) are observed. When the Marangoni driving becomes more intense ($M > 10.75$), the entire flow reverses, and the physical assumption of negative tail-to-nose surface tension gradient is likely to break down.

References

[1] Hadamard J.: Spherical drops, *Comptes Rendus*, **152**: 1735, 1911.
[2] Rybzynski W.: Uber die fortschreitende Bewegung einer Flüssingen Kugel in einem zähen Medium. *Bul l. Acad. Sci. Cracovie*, **1A**: 40–46, 1911.
[3] Levich V.: Physicochemical Hydrodynamics; Prentice-Hall: Englewood cliffs, NJ, 1962.
[4] Bush J.: The anomalous wake accompanying bubbles rising in a thin gap: a forced Marangoni flow. *J. Fluid Mech* **352**: 283–303, 1997
[5] Dangla R., Lee S. and Baroud C. N.: . *Phys. Rev. Lett.* **107**: 124501, 2011.
[6] Thompson B. W.: Secondary flows in a Hele-Shaw cell. *J. Fluid Mech* **31**: 379-395, 1968.